PHYSICAL REVIEW D VOLUME 16, NUMBER 11 1 DECEMBER 1977

Field theories of strong interactions and scaling deviations in deep-inelastic lepton-hadron processes

M. Glück and E. Reya
Institut für Physik, Universität Mainz, 6500 Mainz, West Germany
(Received 8 March 1977)

Scaling deviations of deep-inelastic lepton-hadron reactions are compared with predictions of various theories of strong interactions. It is shown that only asymptotically free theories are compatible with experiment.

I. INTRODUCTION

This is a sequel to our previous investigation on operator mixing and scaling deviations in asymptotically free field theories[1] as well as an extension of a similar investigation done for asymptotically nonfree theories.[2] In our first paper the parton aspects of the underlying theory were not fully taken into account and therefore, although the mixing problem was treated correctly, the input functions used in *ep* scattering could not be used for a simultaneous analysis of *en* or neutrino reactions. In Ref. 1 these input structure functions were in fact *fitted* so as to give optimal agreement with the *ep* data. Here we adopt a different approach and utilize as input functions one of the many parton parametrizations given in the literature. No free parameters will therefore be available except some for the gluon and charmed-quark distributions and obviously the one related to the coupling constant. This will therefore provide a much more stringent test of the strong-interaction field theories, i.e., the theory should succeed (or fail) in *simultaneously* explaining the data for scaling violations in $e(\mu)N$ and $\nu(\bar{\nu})N$ reactions with the *given*, and rather reasonable, parton distributions as input.

Similar investigations were carried out recently for electroproduction[3] and neutrino[4] reactions, however, only for asymptotically free gauge theories (AFGT). Moreover, some plausible assumptions were made in Ref. 3 in order to uniquely determine the input gluon and sea distributions, namely, that at very low values of Q^2 (0.01–0.1 GeV^2, say) the nucleon consists of valence quarks only. We have shown,[2] however, that these assumptions are violated in asymptotically nonfree theories. We therefore prefer, in our present investigation, a more phenomenological attitude toward the input gluon and sea parametrizations. Also in contrast to Ref. 3 we take account of charm production in $e(\mu)N$ reactions and show that observable effects are to be expected and have probably already been seen at presently available energies.

For this purpose we present the full dependence of the structure functions on the momentum transfer Q^2 and not just their average slope (at fixed x) with respect to Q^2, as done in Refs. 2, 3.

In Sec. II we present the general theoretical framework relevant to our analysis. Sections III and IV then specify the details as well as the results for theories with vector gluons and with scalar gluons, respectively. Finally our conclusions are summarized in Sec. V.

II. GENERAL THEORETICAL FRAMEWORK

The moments $\langle F(Q^2)\rangle_n$ of the structure functions $F(x, Q^2)$,

$$\langle F(Q^2)\rangle_n = \int_0^1 dx\, x^{n-2} F(x, Q^2)\,, \tag{2.1}$$

receive contributions from Wilson operators with different flavor content[5,1]

$$\langle F(Q^2)\rangle_n = \langle F_{\rm NS}(Q^2)\rangle_n + \langle F_-(Q^2)\rangle_n + \langle F_+(Q^2)\rangle_n\,, \tag{2.2}$$

with $F_{\rm NS}$ corresponding to the nonsinglet (NS) fermion Wilson operator and with $F_\pm$ corresponding to the two multiplicatively renormalizable singlet operators. These operators have different anomalous dimensions and therefore also predict a different Q^2 behavior of the corresponding moments, namely,

$$\langle F_{\rm NS}(Q^2)\rangle_n = \langle F_{\rm NS}(Q_0^{\,2})\rangle_n e^{-s a_{\rm NS}(n)}\,, \tag{2.3}$$

$$\langle F_\pm(Q^2)\rangle_n = \langle F_\pm(Q_0^{\,2})\rangle_n e^{-s a_\pm(n)}\,, \tag{2.4}$$

with $a_{\rm NS}$, $a_\pm$ linearly related to the anomalous dimensions $\gamma_{\rm NS}, \gamma_\pm$ and with s an increasing function of Q^2 to be further specified later. In order to obtain $\langle F(Q^2)\rangle_n$ or $F(x, Q^2)$, their values at some specific Q^2, say $Q^2 = Q_0^{\,2}$, have to be given separately since these, in contrast to (2.3) and (2.4), *cannot* be calculated from the underlying field theory by perturbative methods. As mentioned in the Introduction we shall express these input functions in terms of parton distributions. In the commonly accepted valence-sea parton model the parton distributions are given by

$$u = u_V + \xi\ , \quad \bar{u} = \bar{d} = s = \bar{s} \equiv \xi\ ,$$
$$d = d_V + \xi\ , \quad c = \bar{c} \equiv \xi'\ , \tag{2.5}$$

where the various distributions are functions of $x = \omega^{-1} = Q^2/2M\nu$ and of Q^2. Then the NS piece F_{NS} in the different reactions is a linear combination of A_3, A_8, and A_{15}, which transform as the third, eigth, and fifteenth basis vectors, respectively, of the adjoint representation[6] of SU(4), each having the same Q^2 dependence as in Eq. (2.3), while the singlet components are given by

$$\langle F_\pm(Q^2)\rangle_n = \left[\begin{pmatrix} 1 - p^-_{11}(n) \\ p^-_{11}(n) \end{pmatrix}\langle A_0(Q_0^2)\rangle_n \mp p^-_{21}(n)\langle G(Q_0^2)\rangle_n\right] e^{-s a_\pm(n)}\ . \tag{2.6}$$

Here the fermionic singlet contribution A_0 and the fermionic NS components $A_{3,8,15}$ are related to the parton distributions through

$$\begin{aligned} A_0 &= u_V + d_V + 6\xi + 2\xi'\ ,\\ A_3 &= u_V - d_V\ ,\\ A_8 &= u_V + d_V\ ,\\ A_{15} &= u_V + d_V + 6\xi - 6\xi'\ . \end{aligned} \tag{2.7}$$

The gluon distribution $G(x, Q^2)$ is generally disregarded in naive parton analyses since it is of no relevance there. Here, however, it enters through Eqs. (2.2) and (2.6) for $Q^2 \neq Q_0^2$ and should therefore also be specified. The influence of $\langle G(Q_0^2)\rangle_n$ comes through its mixing with the fermionic singlet A_0 in Eq. (2.6) via the projection matrices $\hat{P}^\pm$, which project onto the singlet Wilson operators with anomalous dimensions $\gamma_\pm$ through $\hat{\gamma} = \gamma_- \hat{P}^- + \gamma_+ \hat{P}^+$. The anomalous dimensions γ_- and γ_+ are the small and large eigenvalues of $\hat{\gamma}$. This, as well as the relevant matrix elements p^-_{ij} of $\hat{P}^-$, will be specified in Secs. III and IV.

The parton and gluon input ($Q_0^2 = 4$ GeV^2) distributions chosen here are

$$\begin{aligned} u_V(x, Q_0^2) &= 0.594x^{1/2}(1-x^2)^3 + 0.461x^{1/2}(1-x^2)^3 + 0.621x^{1/2}(1-x^2)^7\ ,\\ d_V(x, Q_0^2) &= 0.072x^{1/2}(1-x^2)^3 + 0.206x^{1/2}(1-x^2)^5 + 0.621x^{1/2}(1-x^2)^7\ ,\\ \xi(x, Q_0^2) &= 0.145(1-x)^9\ ,\\ \xi'(x, Q_0^2) &= 0.145(1-x)^{13.5}\ ,\\ G(x, Q_0^2) &= 0.159(1-x^2)^5 + 1.308(1-x^2)^7\ , \end{aligned} \tag{2.8}$$

where for u_V, d_V, and ξ we adopted the parametrization of Barger and Phillips,[7] extracted from eN and νN experiments. The value $Q_0^2 = 4$ GeV^2 corresponds to the average Q^2 of the data. (Any other input parametrization or the data themselves will do as well.) The charmed-quark sea was determined so as to satisfy $\langle\xi'(Q_0^2)\rangle_2 < \langle\xi(Q_0^2)\rangle_2$, a plausible requirement in view of the heaviness of the charmed quarks. A value $\langle\xi'(Q_0^2)\rangle_2 = 0.01$ was chosen, in agreement with the $\langle y\rangle^{\bar{\nu}}$ data at $Q^2 = 4$ GeV^2 and also compatible with the results of Ref. 4. The power 13.5 was chosen so as to guarantee a very little hard ($x \sim 1$) component of charmed partons as well as $\xi'(x=0, Q_0^2) = \xi(x=0, Q_0^2)$, which is plausible since for $x \simeq 0$ one expects only a small SU(4)-symmetry breaking of the sea.

The gluon distribution was determined by the constraints $\langle G(Q_0^2)\rangle_2 = 1 - \langle u_V + d_V + 6\xi + 2\xi'\rangle_2 = 0.475$ from neutrino data, and $\langle G(Q_0^2)\rangle_3 = 0.095$ as argued in Ref. 4; the argument here is that, since $\langle x\rangle_{\text{gluons}} = \langle G\rangle_3/\langle G\rangle_2$ and since the sea quarks originate in pairs from gluons (the latter being mostly emitted by valence quarks), one expects $\langle x\rangle_{\text{sea}} < \langle x\rangle_{\text{gluons}} < \langle x\rangle_{\text{valence}}$. With $\langle x\rangle_{\text{sea}} \simeq 0.1$ and $\langle x\rangle_{\text{valence}} \simeq 0.3$ it is reasonable to choose $\langle x\rangle_{\text{gluons}} = 0.2$, which, together with $\langle G(Q_0^2)\rangle_2 = 0.475$, yields $\langle G(Q_0^2)\rangle_3 = 0.095$. The powers 5 and 7 in Eq. (2.8) for $G(x, Q_0^2)$ were chosen to guarantee that the nucleon contains gluons which are softer than the valence quarks.[8]

Once these input functions are given, their values at arbitrary Q^2 are determined as explained before and by using standard Mellin inversion techniques.[1-3] Then the values of the various deep-inelastic structure functions are given by the standard parton-model formulas. For the neutrino total cross sections a further simplification[4] is adopted by replacing the relevant x and Q^2 integrations over the structure functions $F(x, Q^2)$ by the moments $\langle F(\langle Q^2\rangle)\rangle_2$, with the average $\langle Q^2\rangle$ depending on the reaction energy E through $\langle Q^2\rangle = 2ME\langle xy\rangle$. This is a reasonable approximation since experimentally $\langle xy\rangle$ is almost constant with a value of 0.12 for neutrino reactions and 0.07 for antineutrino reactions. The replacement of integrals over structure functions by lowest moments greatly simplifies the analysis, the errors of this approximation being estimated to be less than 5%.

The charm-production threshold energy was chosen to be $W_{\text{th}} = 6$ GeV, where $W^2 - M^2 = 2MEy(1-x)$ and $y = \nu/E$. For neutrino reactions we take, as in Ref. 4,

$$y_{\text{th}} = \frac{W_{\text{th}}^2 - M^2}{2ME(1-x_0)}\ , \tag{2.9}$$

with $x_0 \simeq 0.2$, so as to be able to replace integrals over structure functions by moments also for the heavy-current piece. This approximation is, again, reasonable since for $x > 0.2$ the relevant sea in Eq. (2.8) is indeed rather small.

III. VECTOR-GLUON THEORIES

The elements of the anomalous-dimension matrix

$$\hat{\gamma} = \begin{pmatrix} \gamma_{FF}^F & \gamma_{FF}^V \\ \gamma_{VV}^F & \gamma_{VV}^V \end{pmatrix} \tag{3.1}$$

are given by[5]

$$\gamma_{FF}^F = \frac{\alpha}{2\pi} C_2(R)\left[1 - \frac{2}{n(n+1)} + 4\sum_{j=2}^{n}\frac{1}{j}\right],$$

$$\gamma_{VV}^V = \frac{\alpha}{2\pi}\left\{C_2(G)\left[\frac{1}{3} - \frac{4}{n(n-1)} - \frac{4}{(n+1)(n+2)} + 4\sum_{j=2}^{n}\frac{1}{j}\right] + \tfrac{4}{3}T(R)\right\},$$

$$\gamma_{VV}^F = -\frac{\alpha}{2\pi}\frac{4(n^2+n+2)}{n(n+1)(n+2)}T(R), \tag{3.2}$$

$$\gamma_{FF}^V = -\frac{\alpha}{2\pi}\frac{2(n^2+n+2)}{n(n^2-1)}C_2(R)$$

with $\alpha = g^2/4\pi$ and g the fermion-gluon coupling constant. For AFGT with color-SU(3) symmetry the group invariants are given by $C_2(G) = 3$, $C_2(R) = \frac{4}{3}$, and $T(R) = \frac{1}{2} \times$ (number of flavors). For Abelian gluon theories $C_2(G) \equiv 0$, $C_2(R) \equiv 1$, and $T(R)$ = (number of different quarks). In our present study of Abelian gluon theories we have set $T(R) = 12$, corresponding to quarks carrying 4 flavors *as well as* 3 colors, where the last property, although not intrinsically needed in Abelian theories, is nevertheless desired in order to guarantee the rate for $\pi^0 \to 2\gamma$ and the other advantages[9] connected with colored quarks.

For AFGT the renormalization-group exponents in Eqs. (2.3), (2.4), and (2.6) are given by $(i = \mathrm{NS}, \pm)$

$$a_i = \gamma_i/(8\pi\alpha b), \quad s = \ln\frac{\ln(Q^2/\Lambda^2)}{\ln(Q_0^{\,2}/\Lambda^2)} \tag{3.3}$$

with Λ to be determined by experiment and where

$$b = \frac{1}{16\pi^2}\left[\tfrac{11}{3}C_2(G) - \tfrac{4}{3}T(R)\right]. \tag{3.4}$$

The γ_i are the following: $\gamma_{\mathrm{NS}} = \gamma_{FF}^F$ and $\gamma_\pm$ are the two eigenvalues of $\hat{\gamma}$ as specified in Sec. II.

For the Abelian vector-gluon theory we have

$$a_i = \gamma_i/2, \quad s = \ln(Q^2/Q_0^{\,2}), \tag{3.5}$$

where the value of α at the ultraviolet (UV) finite fixed point, which now appears in the expression for a_i, has to be determined by experiment. The relevant projection matrix elements in Eq. (2.6) are given by

$$p_{11}^- = \frac{\gamma_{FF}^F - \gamma_+}{\gamma_- - \gamma_+}, \quad p_{21}^- = \frac{\gamma_{VV}^F}{\gamma_- - \gamma_+}. \tag{3.6}$$

The results of these calculations are presented in Figs. 1 and 2. It is seen that AFGT (solid curves) succeed in simultaneously fitting the $e(\mu)N$ and $\nu(\bar{\nu})N$ data[10-13] with a reasonable effective coupling constant

$$\bar{\alpha}(Q^2) = \frac{12\pi}{25\ln(Q^2/\Lambda^2)},$$

corresponding to $\Lambda = 0.5$ GeV. It should be noted that present data allow for slight variations of Λ in the range $0.3\ \mathrm{GeV} \lesssim \Lambda \lesssim 0.7\ \mathrm{GeV}$. Similar values were obtained in Refs. 1, 3, and 4 and are not modified (diminished[14]) by including rescaling effects, as was recently demonstrated by De Rújula, Georgi, and Politzer,[15] who obtained $\Lambda \simeq 0.5$ GeV by studying the SLAC region ($x \gtrsim 0.33$) *with* their ξ variable. That rescaling is unimportant even near the threshold region follows from the rather high values of Q^2 available there. This was further demonstrated by Barbieri, Ellis, Gaillard, and Ross[16] and was already discussed qualitatively in Ref. 17.

The finite steps in Fig. 1 at $Q_{\mathrm{th}}^{\,2} = (W_{\mathrm{th}}^{\,2} - M^2)/(\omega - 1)$ are due to the opening of the charm channel. The magnitude and location of these steps are, for AFGT, not in disagreement with the data whose poorness, however, forbids a conclusive statement as to whether charm production is really indicated in the Fermilab region. One can say, however, that the qualitative agreement with the Fermilab data is improved by including these charm effects in the asymptotically free theory, but only improvements in the statistics of the data as well as a detailed analysis of the produced particles can answer this question more definitely.

From Fig. 2 it is clear that renormalization-group effects in AFGT account fairly well[4] for the y anomaly as well as for the rising of the ratio of total neutrino cross sections $\sigma^{\bar{\nu}}/\sigma^{\nu}$. It is premature to say whether neutrino data as shown in Fig. 2 imply additional quark flavors.[18] One might see an indication for this in the slight discrepancy between the (poor) data for $\langle y\rangle^{\bar{\nu}}$ and $\sigma^{\bar{\nu}}/\sigma^{\nu}$ and the predictions of the four-flavor model with $\Lambda = 0.5$ GeV, but one surely needs to await better data before drawing any final conclusions (especially in view of the experimental ambiguities[13] in normalizing the neutrino fluxes).

Contrary to the success of AFGT, the Abelian vector-gluon theory fails completely in explaining the data for any coupling constant. While a large[19] coupling constant ($\alpha \simeq 0.75$) succeeds fairly well in fitting the SLAC-MIT threshold region ($x \gtrsim 0.5$) in Fig. 1 (dashed-dotted curve), it fails completely to follow the data at $x \lesssim 0.3$ as well as the neutrino data in Fig. 2. In fact, as one sees in Fig. 2 the total-cross-section ratio as well as $\langle y\rangle^{\bar{\nu}}$ become

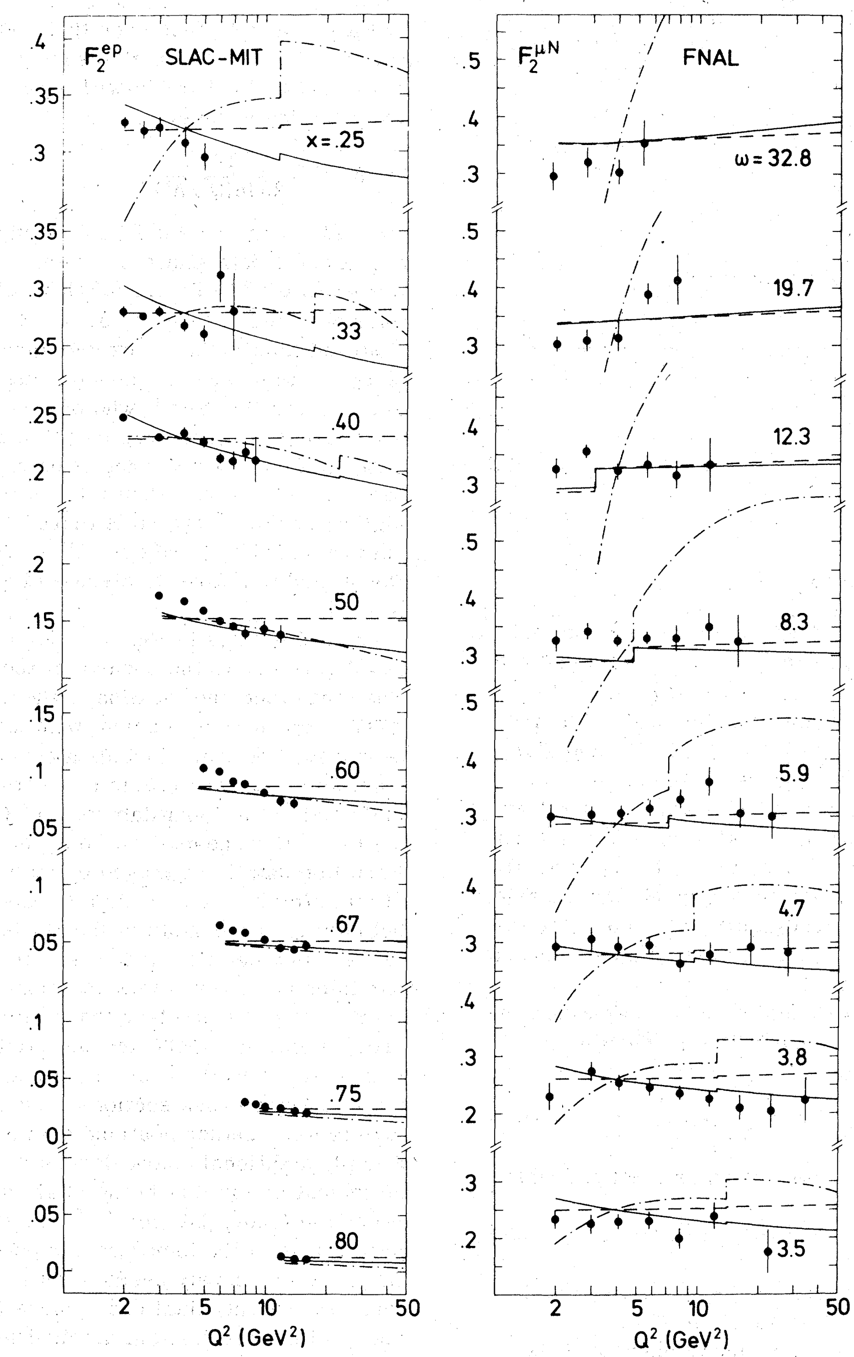

FIG. 1. Comparison of the SLAC-MIT data (Ref. 10) and the isoscalar Fermilab data (Ref. 11) with predictions of vector-gluon theories. Solid curves correspond to AFGT with $\Lambda = 0.5$ GeV; the results of Abelian theories are given by the dashed ($\alpha = 0.01$) and dashed-dotted ($\alpha = 0.75$) curves. Only those data have been used which correspond to $Q^2 \geq 2$ GeV^2 and $W \geq 2$ GeV.

negative around $E \simeq 20$ GeV. This is related to parton distributions becoming negative in this energy (Q^2) range, stressing further the unphysical nature of large fixed points. The upper bound for α is dictated by the requirement $\langle G(Q^2)\rangle_2 < 1$; specifically at $Q^2 \simeq (300\text{ MeV})^2$ one expects[3] $\langle G(Q^2)\rangle_2 \ll 1$, which implies[2] $\alpha \ll 0.2$, i.e., much smaller than the charmonium value.

A small coupling constant ($\alpha \simeq 0.01$), on the other hand, fails to explain the scaling deviations

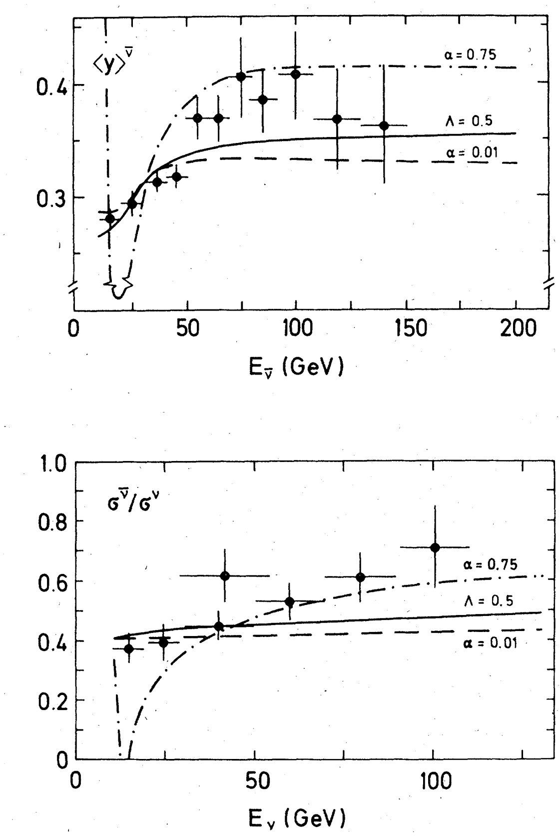

FIG. 2. Predictions of vector-gluon theories for the average value of y for antineutrinos (Ref. 12) and for the ratio of total antineutrino and neutrinto cross sections (Ref. 13), where the notation is as in Fig. 1.

in the SLAC-MIT region as shown by the dashed curves in Fig. 1. Abelian vector-gluon theories are therefore incompatible with the data. They are furthermore also physically unappealing since, as we have shown in Ref. 2, they predict a gluon distribution which is *decreasing* with Q^2 in contrast to what one would expect for gluons radiatively emitted by valence quarks. Quantitatively this can be seen in Fig. 3, where the increasing Q^2 dependence of $G(x,Q^2)$ in AFGT (solid curve) is to be contrasted with the *decreasing* behavior of the Abelian theory (dashed curve) resulting[2] from $\epsilon(Q^2) \equiv \langle u+\bar u+d+\bar d+s+\bar s+c+\bar c\rangle_2$ being smaller than $p_{11}^{-}(n=2)=\frac{6}{7}$.

The Q^2 dependence of the parton and gluon distributions as shown in Fig. 3 are to be contrasted with the Q^2-independent conventional (naive) parton-model distributions. This change with Q^2 or, in neutrino reactions, with the energy $E=\langle Q^2\rangle/2M\langle xy\rangle$ is a further and clear advantage of the field-theoretical approach over the naive parton model, where one is forced by the data to use *different phenomenological* parton parametrizations[20] for low and high neutrino energies. Furthermore one is not confronted with apparent contradictions[21] arising exclusively from (falsely) assuming energy-independent parton distributions.

Finally it should be emphasized that the anomalous dimensions (3.2), as well as those for scalar-gluon theories to be discussed in the next section, have been obtained by lowest-order perturbation theory. One might wonder whether higher-order contributions to γ are indeed negligible in conventional, asymptotically nonfree field theories with a finite ultraviolet fixed point g^*. All calculations concerning these nonfree theories are clearly based on two separate assumptions:

(i) We assume the existence of an ultraviolet fixed point g^*, i.e., $\beta(g^*)=0$, such that the effective coupling constant $g^{*2}/4\pi^2 \ll 1$.

(ii) We assume that near $g=g^*$, $\gamma(g)$ is accurately expressed by leading-order perturbation theory, even though $\beta(g)$ is *not*.

Assumption (i) is necessary in order not to reject *a priori* conventional field theories as possible

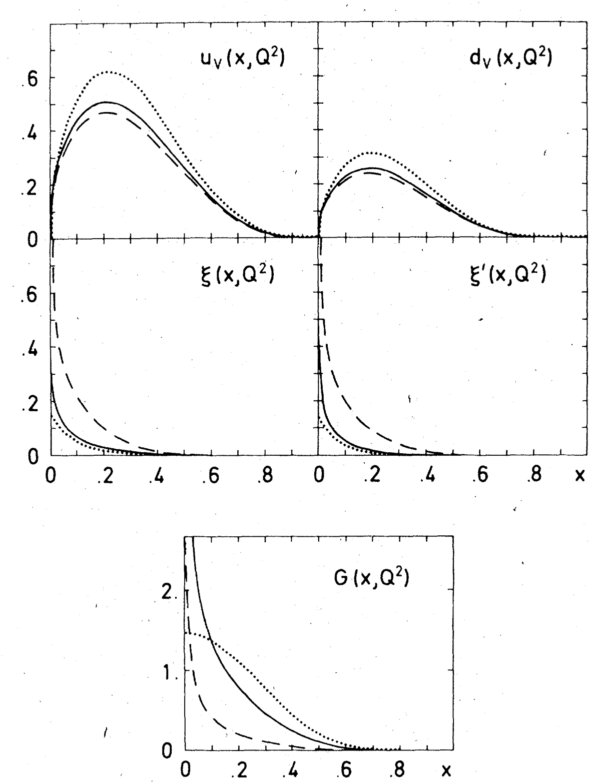

FIG. 3. Parton and gluon distributions for vector-gluon theories. The dotted curves are the input at $Q^2=Q_0^2=4$ GeV^2. The predictions at $Q^2=50$ GeV^2 of AFGT (with $\Lambda=0.5$ GeV) are given by the solid lines, and of Abelian theories (with $\alpha=0.75$) by the dashed lines.

candidates for explaining (perturbatively) the experimentally observed *small* scaling violations. Any quantitative calculation clearly requires in addition assumption (ii), i.e., $\gamma(g^*) = \sum_k c_k g^{*2k} \simeq c_1 g^{*2}$, although higher-order terms are certainly important in the perturbative expansion of the Callan-Symanzik function $\beta(g) = \sum_k b_k g^{2k+1}$ at $g = g^*$ since cancellations between *different* orders are

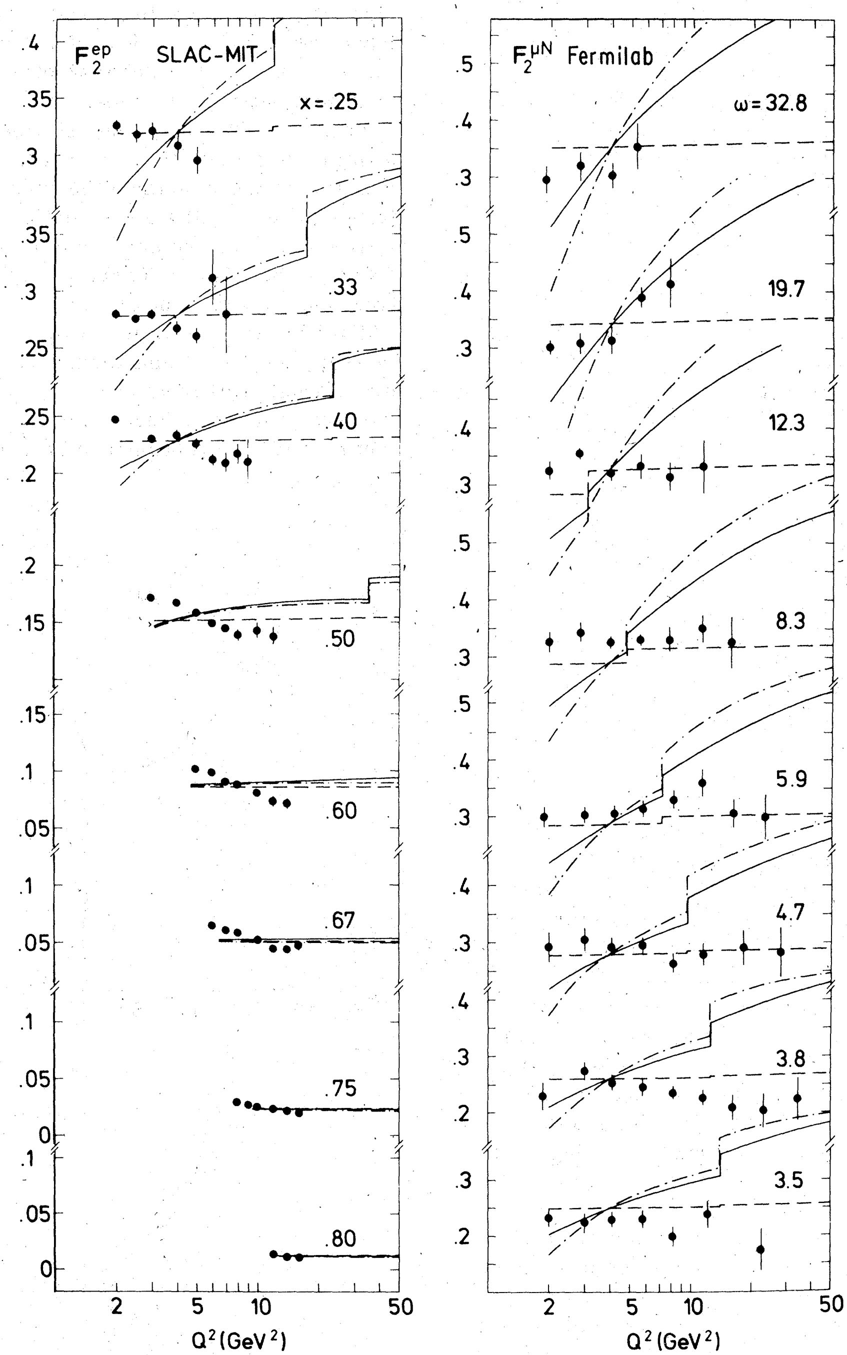

FIG. 4. Comparison of the data (as in Fig. 1) with the predictions of scalar-gluon theories. Dashed ($\alpha = 0.01$) and dashed-dotted ($\alpha = 0.75$) curves correspond to non-Abelian theories, while the results of the Abelian theory are given by the solid curves ($\alpha = 0.075$) and the ones for $\alpha = 0.001$ coincide with the dashed lines.

needed to get $\beta(g^*)=0$. It should be emphasized that only an effective coupling constant $g^{*2}/4\pi^2 \ll 1$ has been used throughout our analysis.

IV. SCALAR-GLUON THEORIES

Here again the gluon ϕ may belong to the adjoint representation of SU(3) (non-Abelian scalar gluons) or to the singlet representation (Abelian scalar gluons). The number of different quarks is taken to be 12 in *both* cases as in Sec. III, but again the results are not very sensitive to this special choice. The anomalous-dimension matrix is, in an obvious notation, given by[22]

$$\gamma^F_{FF}=\frac{\alpha}{4\pi}C_2(R)\left[1-\frac{2}{n(n+1)}\right],$$
$$\gamma^\phi_{\phi\phi}=-\gamma^F_{\phi\phi}=\frac{3\alpha}{\pi}T(R)\,, \qquad (4.1)$$
$$\gamma^\phi_{FF}=-\frac{\alpha}{\pi}C_2(R)\frac{1}{n(n+1)}\,,$$

where $C_2(R)=\frac{4}{3}$, $T(R)=\frac{1}{2}\times$ (number of flavors) for the non-Abelian case, and $C_2(R)\equiv 1$, $T(R)=$ (number of different quarks) for the Abelian case. In both cases the renormalization-group exponents are given by Eq. (3.5) while the projection matrix elements are the same (with $V\to\phi$) as in Eq. (3.6).

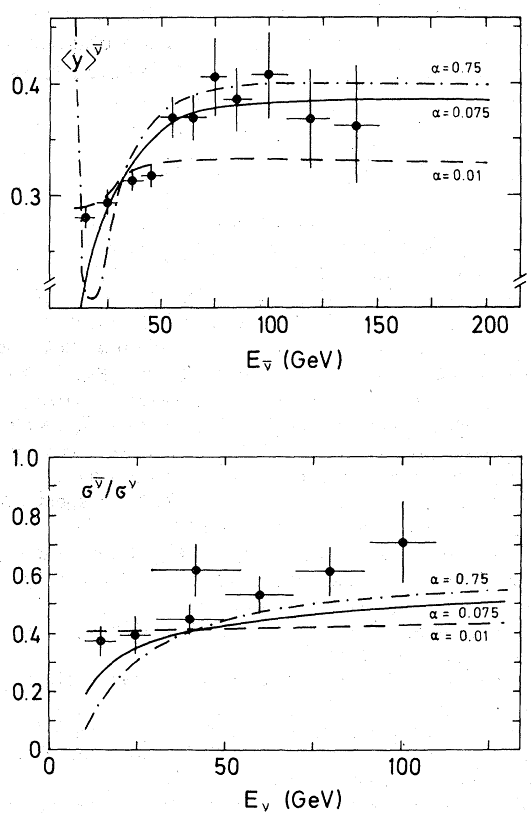

FIG. 5. Comparison of the neutrino data (as in Fig. 2) with scalar-gluon theories using the same notation as in Fig. 4.

The results of these calculations are presented in Figs. 4 and 5. It is seen that for scalar-gluon theories the situation is similar to the Abelian vector-gluon case, but the agreement with experiment is even worse. Here, the theoretical predictions fail to reproduce the *qualitative* features of the data even in the threshold region ($x>0.2$) for *any* choice of α; although the data show a clear decreasing-Q^2 behavior of $F_2(x,Q^2)$ near threshold, Yukawa theories always yield a positive slope for F_2 at $x\lesssim 0.8$ as shown in Fig. 4 (see also Ref. 2). This conclusion is in contradiction to the results of Tung,[23] who states that with present eN and μN experiments a distinction between finite fixed-point theories and AFGT is impossible. In Ref. 23, however, not all features of the theories to be compared with were considered, expecially not the ones related to operator-mixing effects. Instead, a *single* effective anomalous dimension was introduced which was expected to simulate the essential mixing features. This was undertaken by modifying the anomalous dimension of the diagonal fermionic Wilson operator, $\gamma^F_{FF}\sim 1-2/n(n+1)$, into $\gamma_{\rm eff}=2A[1-6/n(n+1)]$ so as to guarantee the conservation of the energy-momentum tensor.[24] Agreement with the threshold data was obtained[23] for $A=0.25$ which corresponds to $\alpha\simeq 5$. With this large value of α, however, it is impossible to reproduce[2] the small-x (Fermilab) data. Moreover, large values of α are excluded by requiring $\langle G(Q^2)\rangle_2\ll 1$ at $Q^2\simeq(300\text{ MeV})^2$, which implies[2] $\alpha\ll 0.2$ for non-Abelian scalar theories, and $\alpha\ll 0.03$ for Abelian scalar theories.

We have already emphasized in Sec. III that finite fixed-point theories predict for the quark-gluon content of the nucleon a qualitatively very different behavior[2] than AFGT. The predictions in Fig. 4 and those of Abelian vector-gluon theories in Fig. 1 (dashed and dashed-dotted curves) clearly show that the area under F_2^{eN}, i.e.,

$$\langle F_2^{eN}(Q^2)\rangle_2=\tfrac{5}{18}p_{11}^-(2)+\tfrac{5}{18}[\epsilon(Q_0^2)-p_{11}^-(2)]e^{-sa_+(2)}$$
$$-\tfrac{1}{3}\langle\xi(Q_0^2)-\xi'(Q_0^2)\rangle_2 e^{-sa_{NS}(2)}\,, \qquad (4.2)$$

increases with Q^2 since $p_{11}^-(2)>\epsilon(Q_0^2)\simeq 0.5$ for all field theories[2] except AFGT. Thus, starting from $\langle F_2^{eN}(Q_0^2)\rangle_2\simeq 0.14$, this area must rapidly approach from *below* its asymptotic value $\frac{5}{18}p_{11}^-$ ($=\frac{5}{21}$, $\frac{15}{56}$, and $\frac{60}{217}$ for Abelian vector-gluon, non-Abelian scalar-gluon, and Abelian scalar-gluon theories, respectively), whereas for AFGT ($p_{11}^-<\epsilon$) this area of 0.14 approaches $\frac{5}{18}p_{11}^-=\frac{5}{42}=0.119$ *slowly* from above. This is the very reason why finite fixed-point theories exhibit a Q^2 dependence so much different from AFGT.

V. CONCLUSIONS

We have shown that, contrary to common belief, AFGT *can* be distinguished from finite ultraviolet fixed-point theories. The distinction is possible *only* if mixing effects are *fully* taken into account. It turns out that only AFGT can simultaneously explain all existing data on scaling deviations in deep-inelastic lepton-hadron processes. This is accomplished by using commonly accepted parton distributions combined with their Q^2 modifications due to renormalization effects, with a value of the running coupling constant corresponding to $\Lambda \simeq 0.5$ GeV, in reasonable agreement with estimates from the charmonium model. No definite indication, however, is yet available for charm-production effects by comparing even the detailed (i.e., as contrasted to the average slope results of Ref. 3) predictions of AFGT with the Fermilab data. Improved experiments should settle this question. Taking momentum-*dependent* parton distributions, one is furthermore not confronted with apparent inconsistencies[21] arising exclusively from assuming naive Q^2- independent parton distributions.

That the present data on $\sigma^{\bar{\nu}}/\sigma^{\nu}$ imply additional quark flavors seems premature to conclude. One might see an indication for this in the slight discrepancy between the data and the renormalization-group improved four-flavor model, but one certainly needs to await better data before drawing any final conclusions.

In contrast to the success of AFGT, we have dedemonstrated that renormalization effects of asymptotically *nonfree* theories of strong interactions (i.e., Abelian gluon theories as well as non-Abelian and Abelian Yukawa theories) are incompatible with experiment and with physical expectations of Q^2 dependences of parton and gluon distributions.

That field-theoretic Q^2 modifications of parton distributions and of the quark-gluon coupling constant are also important in high-p_T hadron reactions was recognized by many authors,[25] who pointed to significant modifications of naive scaling and counting rules.[26] The question as to whether these modifications are compatible with AFGT or fixed point theories was, however, not definitely answered in purely hadronic processes due to the crudeness of the analysis and to uncertainties of the underlying parton mechanisms. This should be contrasted with the theoretically much more definite picture (i.e., Wilson expansion) of lepton-hadron physics. A careful field-theoretical analysis of various parton reaction mechanisms should therefore prove rewarding not only in distinguishing between AFGT and ultraviolet fixed-point theories on a purely hadronic level, but also in delineating the relevant parton scattering diagrams responsible for high-transverse-momentum processes.

---

[1]M. Glück and E. Reya, Phys. Rev. D 14, 3034 (1976).

[2]M. Glück and E. Reya, Phys. Lett. 69B, 77 (1977).

[3]G. Parisi and R. Petronzio, Phys. Lett. 62B, 331 (1976).

[4]G. Altarelli, R. Petronzio, and G. Parisi, Phys. Lett. 63B, 183 (1976).

[5]D. J. Gross and F. Wilczek, Phys. Rev. D 9, 980 (1974); H. Georgi and H. D. Politzer, *ibid.* 9, 416 (1974).

[6]The discussion here concerns the *flavor*-SU(4) group.

[7]V. Barger and R. J. N. Phillips, Nucl. Phys. B73, 269 (1974). Our distributions are x times the ones given by Barger and Phillips.

[8]These gluon and sea parametrizations are consistent with hadron constituent counting rules [G. R. Farrar, Nucl. Phys. B77, 429 (1974); J. F. Gunion, Phys. Rev. D 10, 242 (1974); M. B. Einhorn and S. D. Ellis, *ibid.* 12, 2007 (1975)].

[9]H. Fritzsch, M. Gell-Mann, and H. Leutwyler, Phys. Lett. 47B, 365 (1973).

[10]R. E. Taylor, in *Proceedings of the 1975 International Symposium on Lepton and Photon Interactions at High Energies, Stanford, California*, edited by W. T. Kirk (SLAC, Stanford, 1976), p. 679; E. M. Riordan *et al.*, SLAC Report No. SLAC-PUB-1634, 1975 (unpublished).

[11]C. Chang *et al.*, Phys. Rev. Lett. 35, 901 (1975). Uncertainties of 10% are ascribed to the absolute normalization of $F_2 = \nu W_2(x, Q^2)$, since this experiment does not measure the structure function directly but extracts the (x, Q^2) dependence through a Monte Carlo simulation of SLAC-MIT data.

[12]A. Benvenuti *et al.*, Phys. Rev. Lett. 36, 1478 (1976).

[13]A. Benvenuti *et al.*, Phys. Rev. Lett. 37, 189 (1976).

[14]Recently a much smaller value of Λ ($\Lambda \simeq 0.05$ GeV) was obtained by P. W. Johnson and W. K. Tung [Nucl. Phys. B121, 270 (1977)], who studied the Fermilab region $x < 0.3$ with the help of a *single* effective anomalous dimension. However, the residue of their pole at $n = 0$ is $\frac{48}{25}$, while the theoretically predicted residues at $n = 0$ of a_{NS}, a_-, and a_+ are $-\frac{8}{25}$, $\frac{4}{25}$, and $\frac{24}{25}$, respectively. This overestimate of the pole at $n = 0$, which is very influential in the Fermilab region (Ref. 1), necessitates a compensating underestimate of $\bar{\alpha}$ by a factor of 2, which explains the discrepancy.

[15]A. De Rújula, H. Georgi, and H. D. Politzer, Phys. Lett. 64B, 428 (1976).

[16]G. Barbieri, J. Ellis, M. K. Gaillard, and G. G. Ross, Nucl. Phys. B117, 50 (1976).

[17]M. Glück and E. Reya, Phys. Lett. 64B, 169 (1976).

[18]R. M. Barnett, H. Georgi, and H. D. Politzer, Phys. Rev. Lett. 37, 1313 (1976).

[19]"Large" and "small" are to be understood with respect to the charmonium value $\alpha \simeq 0.2$.

[20]V. Barger, R. J. N. Phillips, and T. Weiler, Nucl.

Phys. B102, 439 (1976).

[21]V. Barger, R. J. N. Phillips, and T. Weiler, Phys. Rev. D 14, 1276 (1976).

[22]D. Bailin and A. Love, Nucl. Phys. B75, 159 (1974).

[23]W. K. Tung, Phys. Rev. Lett. 35, 490 (1975).

[24]Note, however, that $\gamma_{\rm eff}(n=1)\neq 0$ and therefore does not correctly simulate charge, strangeness, and baryon number conservation.

[25]S. D. Ellis, Phys. Lett. 49B, 189 (1974); R. F. Cahalan, K. A. Geer, J. Kogut, and L. Susskind, Phys. Rev. D 11, 1199 (1975); R. C. Hwa, A. J. Spiessbach, and M. J. Teper, Phys. Rev. Lett. 36, 1418 (1976); A. V. Efremov, Phys. Lett. 62B, 173 (1976); M. Glück, Mainz Report No. MZ-TH 76/8 (unpublished).

[26]D. Sivers, S. J. Brodsky, and R. Blankenbecler, Phys. Rep. 23C, 1 (1976), and references therein.